Poll Res. 40 (4): 1589-1600 (2021)

ISSN 0257–8050

ADSORPTION OF HEAVY METALS FROM CONTAMINATED WATER ON Fe_2O_3/ SiO_2 NANOCOMPOSITE AND NATURAL SILICA RICE HULL-BASED AND INVESTIGATE THEIR EFFECTS ON BLOOD BIOMARKERS AND RENAL TOXICITY IN RATS

SOHEIR N. ABD EL-RAHMAN[1*], SAAD A. MAHGOUB[1], AMAL M. H. ABDEL-HALEEM[1*] AND AFAF A. SHAABAN[2]

[1]Crops Technology Research Department, Food Technology Research Institute (FTRI), Agricultural Research Centre, Al Giza-Cairo, Egypt*

[2]Forensic Medicine and Clinical Toxicology Department, Faculty of Medicine for Girls, Al-Azhar University Egypt;

(Received 10 September, 2021; accepted 27 October, 2021)

ABSTRACT

The detection of heavy metals in industrial effluent and some sectors of the global drinking water supply stands in direct opposition to the limits set by the regulatory authorities and the recommended Guidelines by the World Health Organization. Rice husk, as underutilized agricultural biomass, could be transferred into a promising low-cost adsorbent for removing heavy metals as it is abundant in nature, from a biogenic source, and requires little processing. In the present study, silica and Fe_2O_3 silica nanocomposite were prepared from rice husk and used to clean contaminated water with a heavy metal mixture. Silica 0.5 and 1% exhibited up to 97.05 and 100% removal for Zn^{2+}, Fe^{2+}, and Ni^{2+}, respectively, as they were affected by silica cristobalite amorphous microstructures and the non-uniform pore sizes. Silica 0.5% adsorbed more Mn^{2+} (29.45 mg) and Fe^{2+} (54.02 mg) than 1% silica. Fe_2O_3/silica nanocomposite 1% showed a specific selectivity to bind Hg^{2+} with a maximum adsorption removal of 40.42% and adsorption capacity of 0.02 mg/ g. Serum urea, creatinine, and uric acid in rats exposed to drinking water cleaned with 0.5, 1% silica exhibited close $p \leq 0.05$ results to the normal values, and kidney histopathological examinations do not exhibit any sign of nephrotoxicity.

KEY WORDS : Rice hull ash, Silica nanocomposites, Water pollution, EDX-microelement composition, Adsorption capacity and efficiency, Kidney failure

INTRODUCTION

Heavy metals are elements having atomic weights from 63.5 to 200.6, and a specific gravity > 5.0, they are generally referring to metals and metalloids such as Manganese (Mn^{2+}), Iron (Fe^{2+}), Nickel (Ni^{2+}), Mercury (Hg^{2+}), and Lead (Pb^{2+}) (Aliyah, 2012). The heavy metals are usually discharged from urbanization such as nuclear, metallurgical, tannery, mining, cosmetics, insecticides, photography, textiles, paints, dyes, and battery industries. They get accumulated both in underground and surface water, different parts of crops irrigated with contaminated water, and also in aquatic living animals (Ligate and Mdoe, 2015; Rehman *et al.*, 2018; Khan *et al.*, 2020). Small quantities of Fe^{2+} and Mn^{2+} (sometimes called trace elements) are essential for nutrition and health considerations. However, large concentrations of heavy metal did not degrade and accumulated in the living system, which ultimately leads to potential health risks and ecological disturbances. Moreover, prolonged exposure to heavy metals may substitute calcium by Pb^{2+}, zinc by Cd^{2+} and trace elements by Al^{2+}. Furthermore, heavy metals react with oxygen and chloride compounds and expend their toxic effects in the human system (Aliyah, 2012; Rehman *et al.*, 2018). Pb^{2+} can cause headache, irritability, cognitive and

***Corresponding author's email:** soheirkenawy@yahoo.com, amalefsic@yahoo.com
Amal M. H. Abdel-Haleem ORCID: https://orcid.org/0000-0001-9912-3390

behavioral impairments, anemia, abdominal pains, blood pressure, nephritic damage, stomach and lungs cancers, gliomas, and reproductive system toxicity. Hg^{2+} can cause many harmful health effects depending upon its form (metallic, inorganic, organic) and the level of exposure. At high levels of contamination, Hg^{2+} can cause nerve and kidney malfunctions and some neurotoxicity symptoms. Experimental animals exposed to mercury vapor showed obscure signs of pathological changes, cellular degeneration, brain necrosis, and suppressing natural killer cells. Meanwhile, Fe^{2+} in drinking water after long-term exposure may cause nephritic disease, cancer, and anemia, along with metabolism disorders. Also, Mn^{2+} in drinking water can cause Manganism and Alzheimer's. In addition, the Ni^{2+} -sulfate and Ni^{2+} chloride ingestion can cause severe cardiac arrest (Aliyah, 2012; Jaishankar *et al.,* 2014; Abd El-Rahman *et al.,* 2016; Reda *et al.,* 2018; Nguyen, 2019).

Many experimental studies using animal trials showed a synergic effect between heavy metals exposure and renal failure associated with severe physiological and histological alterations. Also, the complete blood count (CBC) detected many abnormalities including, stress enzyme leakage into the bloodstream as affected by the redox reactions and the production of reactive oxygen species with a clear sign of oxidative damage in renal tissues (Abd El-Rahman *et al.,* 2016; Wasana *et al.,* 2017; Rehman *et al.,* 2018).

The detection of heavy metals in industrial effluent and some sectors of the global drinking water supply stands in direct opposition to the limits set by the regulatory authorities and the recommended Guidelines for Drinking Water Safety by the World Health Organization (WHO, 2006). That has raised concerns for the demand for water pollution control, especially with the intensification of global trends such as urbanization, deforestation, and climatic change (World Water Development Report, 2018). Therefore many efforts have been developed to remove heavy metals from water streams using various techniques, particularly the adsorption one. The adsorption technique is a promising technique of removal of heavy metals due to its high efficiency, easy operation, cost-effectiveness, and environmental-friendly nature (Candido *et al.,* 2021).

Rice husk is a by-product of the rice milling industry; it represents ~ 20% of whole milled rice. Internationally, the annual production of rice husk is ~ 100 million tons (Ong *et al.,* 2019), In Egypt, rice production is estimated at 4.5 million tons (FAOSTAT, 2019), and then the volume of rice husk is about one million tons with a silica content of about 10%. However, this volume of rice husks is far in more than any local uses and poses environmental and disposal problems. It would be added value to transform this rice husk as underutilized agricultural biomass into a promising low-cost adsorbent, as it is abundant in nature, from a biogenic source, and requires little processing (Vieira *et al.,* 2014; Ligate and Mdoe, 2015). The rice hull ash could be obtained after burning rice husk at 600° C with a silica (SiO_2) content of 94.5–96.34% (Masoud *et al.,* 2016). It is worth mentioning that the mineral ash SiO_2 is a promising adsorptive material due to its porous structure (10–75 μm) and large surface area (50,000 m^2/kg) with high affinity and selectivity towards heavy metals; this is because of the presence of binding groups on its surface (Siddique and Cachim, 2018; Nguyen, 2019). It's worth more producing silica nanocomposite from rice ash SiO_2 to increase the crystallinity and the structural integrity and to be more economical and environmentally alternative than synthesized or commercial silica nanoparticles, which may not be sustainable and not match the cost requirement (Wang *et al.,* 2012; Dang *et al.,* 2017). Silica nanocomposite can be prepared by the sol-gel methodology from rice husk ash using metal oxides such as Fe_2O_3 as supported oxide. The Fe_2O_3 is a more attractive alternative adsorbent for water treatment as it is cost-effective and non-toxic. The physicochemical properties of the Fe_2O_3/SiO_2 nanocomposite are superior and can be used as adsorbents for a wide variety of reactions (Nguyen *et al.,* 2019 8; Ramutshatsha-Makhwedzha *et al.,* 2019; Agi *et al.,* 2020).

Accordingly, the present research work were aimed to (i) transfer rice husk, as underutilized agricultural biomass, into promising adsorbents: silica and Fe_2O_3 silica nanocomposite at concentrations of 0.5, 1%, for the cleaning of contaminated water with a heavy metal mixture (Mn^{2+}, Fe^{2+}, Ni^{2+}, Hg^{2+}, and Pb^{2+}) against Tetraethyl orthosilicate (TEOS) and Fe_2O_3 / TEOS nanocomposite; (ii) assign the adsorption efficiencies and capacities of the prepared adsorbents via the scanning electron microscopy (SEM) and energy-dispersive X-ray spectroscopy (EDX) and then (iii) use an animal trial to investigate the health effects of different water treatments on blood biomarkers and

renal histology of male rats.

MATERIALS AND METHODS

Materials

The rice hull was obtained from the Experimental Farm of Sakha Agricultural Research Station, Agricultural Research Centre, Kafr El Sheikh Governorate, Egypt. Synthetic or commercial silica: Tetraethyl orthosilicate (TEOS) with purity e"99.0% (GC) was purchased from Sigma-Aldrich, St. Louis, MO, USA. Iron (III) chloride hexahydrate $FeCl_3 \cdot 6H_2O$, Lead (II) acetate trihydrate $Pb(CH_3COO)_2 \cdot 3H_2O$, Manganese (II) chloride tetrahydrate $MnCl_2 \cdot 4H_2O$, Nickel(II) chloride hexahydrate $NiCl_2 \cdot 6H_2O$, and Mercury(II) chloride $HgCl_2$ were obtained from Fluka Chemicals Corporation, St. Louis, USA. Distilled water was purified using the Millipore water purification system, Bedford, MA, USA. All other chemicals and reagents were of analytical grade.

Preparation of natural silica and Fe_2O_3 silica and Fe_2O_3 TEOS nanocomposites

The rice hull biomass was cleaned and rinsed with purified water, dried at 155°C for 48 h, and then furnace for five hours at 600°C to get rice hull ash. Natural silica was prepared from rice hull ash using alkali solubilization, followed by acid precipitation according to the method described by Kamath and Proctor (1998). The rice hulls were dissolved in 1 M NaOH solution and boiled for one hour in a covered Erlenmeyer flask with constant stirring. The solution was flittered then a sol-gel method was performed to prepare silica nanocomposite using SiO_2/ Fe_2O_3 ratio of 70:30 at pH < 2 to prevent precipitation of Fe_2O_3. The obtained xerogels were dried at 100 °C and furnace at 600 °C for one hour. The TEOS nanocomposite was prepared by mixing the TEOS with an aqueous solution of $FeCl_3 \cdot 6H_2O$ in acidified water (HCl) containing EtOH, according to Hrianca *et al.* (2000). The TEOS solution was filtrated then the above-mentioned sol-gel method described by Kamath and Proctor (1998) was performed to obtain the TEOS nanocomposite.

Scanning electron microscopy (SEM)

The microstructure of natural, synthetic, and nanocomposite silica was examined by a scanning electron microscope JEOL, JSM-5200, Tokyo, Japan. The samples were sputter-coated with gold at a vacuum evaporator from 5 to 15 kV accelerating voltage and magnification power of 750-6,000×.

Preparation of the drinking water contaminated with heavy metals

The drinking water contaminated with heavy metals, which included Mn^{2+}, Fe^{2+}, Ni^{2+}, Hg^{2+}, and Pb^{2+}, was prepared by dividing the molecular weight of heavy metal compound by the molecular weight of each metal according to Nwokocha et al. (2010). To avoid precipitation, each heavy-metal was separately dissolved in 1000 mL of purified distilled water as a stock solution. Before use, 200 mL of this solution was mixed with 20 L purified distilled water to obtain 20 L of contaminated water contained the sum of five heavy metals at final working concentrations illustrated in Table 1. Five liters of the working solution were cleaned using each of 2.5; 5 g pre-activated (120° C for 2 hr) natural, synthetic, and nanocomposite silica. The drinking solutions were settled for 24 hr, and then filtrated and used for microelement analysis and biological assay. The solutions were freshly prepared each week to avoid heavy metals precipitation.

Energy-dispersive X-ray spec-troscopy (EDX)

Different water samples (purified, contaminated, and cleaned with natural, synthetic, and nanocomposite silica) were exposed to the microelement analysis using the Energy-dispersive X-ray spectroscopy (EDX) to detect the heavy quantitatively. The EDX model was INCA Sight Oxford equipped with a scanning electron microscope (JEOL, JSM-5500 LV). The mode of

Table 1. The contents and concentrations of the heavy metals in the contaminated drinking water

Compound	M. wt compounds (g/ mol)	M. wt heavy metal (g/ mol)	weight (g)	Final concentrations (mg/ L)
$MnCl_2 \cdot 4H_2O$	197.92	54.94	3.60	1000
$FeCl_3 \cdot 6H_2O$	270.30	55.85	4.84	1200
$NiCl_2 \cdot 6H_2O$	237.69	58.69	4.05	100
$HgCl_2$	271.5	201	1.35	10
$Pb(CH_3COO)_2 \cdot 3H_2O$	379.33	207.2	1.83	100

analysis was Window Integral, the detection limit was 0.1%, scan time was 200 seconds, and scan dimensions were 20 x 300 x 250 μm.

The adsorption capacity and efficiency of natural, synthetic, and nanocomposite silica for heavy metals

The adsorption efficiency (AE) for heavy metals with natural, synthetic, and nanocomposite silica was calculated in percentages (%) at fixed conditions at 37±2° C after 24 hr of water cleaning following equation 1:

$$AE\% = \frac{(C-T)}{C} \times 100 \quad .. (1)$$

Where C is the concentrations of heavy metals (mg/l) in contaminated water; T is the concentrations of the heavy metals (mg/l) after the water cleaning with natural, synthetic, and nanocomposite silica.

The adsorption capacity (AQ), which refers to the amount of heavy metal absorbed per unit mass of natural, synthetic, and nanocomposite silica, was calculated (mg/g) at fixed conditions at 37±2° C after 24 hr of water cleaning following equation 2.

$$AQ\ (mg/g) = \frac{(C-T)V}{m} \times 100 \quad .. (2)$$

Where C is the concentrations of heavy metals (mg/l) in contaminated water; T is the concentrations of the heavy metals (mg/l) after 24 of the water cleaning; V is the volume of the solution (L); m is the mass of adsorbent 5 and 10 g).

Animals and Experimental Design Protocol

Eight-week- male Wistar rats weighing 180±20 g were obtained from Experimental Laboratory Animal Unit, Food Technology Research Institute, Agriculture Research Center, Al Giza, Egypt. The animals were kept at constant room temperature 25±5° C with 12 h of light/ dark cycles. During the acclimatization period, all rats had access to distilled water *ad libitum* and were received a standard laboratory chow prepared with the recommended daily dose for each nutrient according to the National Research Council (1995). Then rats were divided into ten homogenous groups, each of six, and then exposed to oral administration of different water treatments for ten weeks according to the following protocol:

Group 1: fed normal rat chow+ purified distilled water *ad libitum*

Group 2: fed normal rat chow + contaminated drinking water with heavy metals.

Group 3: fed normal rat chow + 0.5% natural silica SiO_2 + contaminated drinking water with heavy metals.

Group 4: fed normal rat chow + 1% natural silica SiO_2 + contaminated drinking water with heavy metals

Group 5: fed normal rat chow + 0.5% synthetic silica TEOS + contaminated drinking water with heavy metals.

Group 6: fed normal rat chow+ 1% synthetic silica TEOS + contaminated drinking water with heavy metals

Group 7: fed normal rat chow+ 0.5% natural Fe_2O_3/ SiO_2 nanocomposite+ contaminated drinking water with heavy metals

Group 8: fed normal rat chow+ 1% natural Fe_2O_3/ SiO_2 nanocomposite + contaminated drinking water with heavy metals

Group 9: fed normal rat chow+ 0.5% synthetic Fe_2O_3/ TEOS nanocomposite + contaminated drinking water with heavy metals

Group 10: fed normal rat chow+ 1% synthetic Fe_2O_3/ TEOS nanocomposite + contaminated drinking water with heavy metals

Biochemical assays

Rats were sacrificed, and blood samples were collected via cardiac puncture and separated into the serum. Serum urea, creatinine, and uric acid were quantified according to the manufacturer's instructions (Bio Diagnostic Company, Dokki, Al-Giza, Egypt).

Histopathological examination

The renal tissues were fixed in 10% neutral formaldehyde and dehydrated with a gradient sequence of aqueous EtOH from 70 to 100%. After that, the dehydrated tissues were embedded into the paraffin, cut into 4-5 μm sections, and then stained with Hematoxylin dye (H&E Staining), according to Suvarna *et al.* (2018). Careful examination of the stained sections was made using a DM750 light microscope, Leica Microsystems IR GmbH, Switzerland, to identify the histopathological alterations induced by different treatments.

Statistical analysis

The data of this study were analyzed using

computer software Jandel Sigma Stat Statistical Software version 2.0 for Windows. An analysis of variance (ANOVA) using a One- Way completely randomized design followed by Fischer's test at $P \leq 0.05$, to compare between means.

RESULTS AND DISCUSSION

The Morphological structure of natural, synthetic, and nanocomposite silica

Figure 1 (a-d) represents the morphological structures of natural, synthetic, and nanocomposite silica. The natural silica (Fig. 1a) exhibited a cristobalite amorphous form with traces of crystalline quartz. The non-uniform particle size was due to the high burning temperature of the rice hull (Thiedeitz *et al.*, 2020). In addition, some particles can be seen agglomerated and stuck to each other due to the high surface energyand free silanol groups (Si—OH) on the natural silica surface (Basri *et al.*, 2020). The high concentrations of Si—OH groups coupled with ordered cristobalite amorphous structures, and the non-uniform pore sizes, make natural silica efficient sorbent for heavy metals in polluted water (Hu *et al.*, 2020). After sol-gel preparation, the natural Fe_2O_3/ SiO_2 nanocomposite (Fig. 1b) was not relatively different from that of the original natural silica. The microstructure became immense irregular, with expander particle size distribution and more agglomerations (Palanivelu *et al.*, 2016 30). The agglomeration referring to the aggregation of Fe_2O_3 on its surface as a result of Van der Waals forces and later that may decrease the adsorption efficiency of the natural Fe_2O_3/ SiO_2 nanocomposite (Ramutshatsha-Makhwedzha *et al.*, 2019). The synthetic TEOS (Fig. 1c) exhibited silica sand flaky aggregates with sub-angular to angular shapes and sharpened edges. Moreover, the microstructure of the synthetic TEOS showed less mount of agglomerations. After sol-gel preparation, the synthetic Fe_2O_3/ TEOS nanocomposite (Fig. 1d) exhibited a fully modified and uniform crystalline structure. This structure is beneficial for the surface activity of the composite where it increases the surface to volume ratio, eventually increase the interaction with heavy metal molecules. In our previous work (Reda *et al.*, 2018), we analyzed the

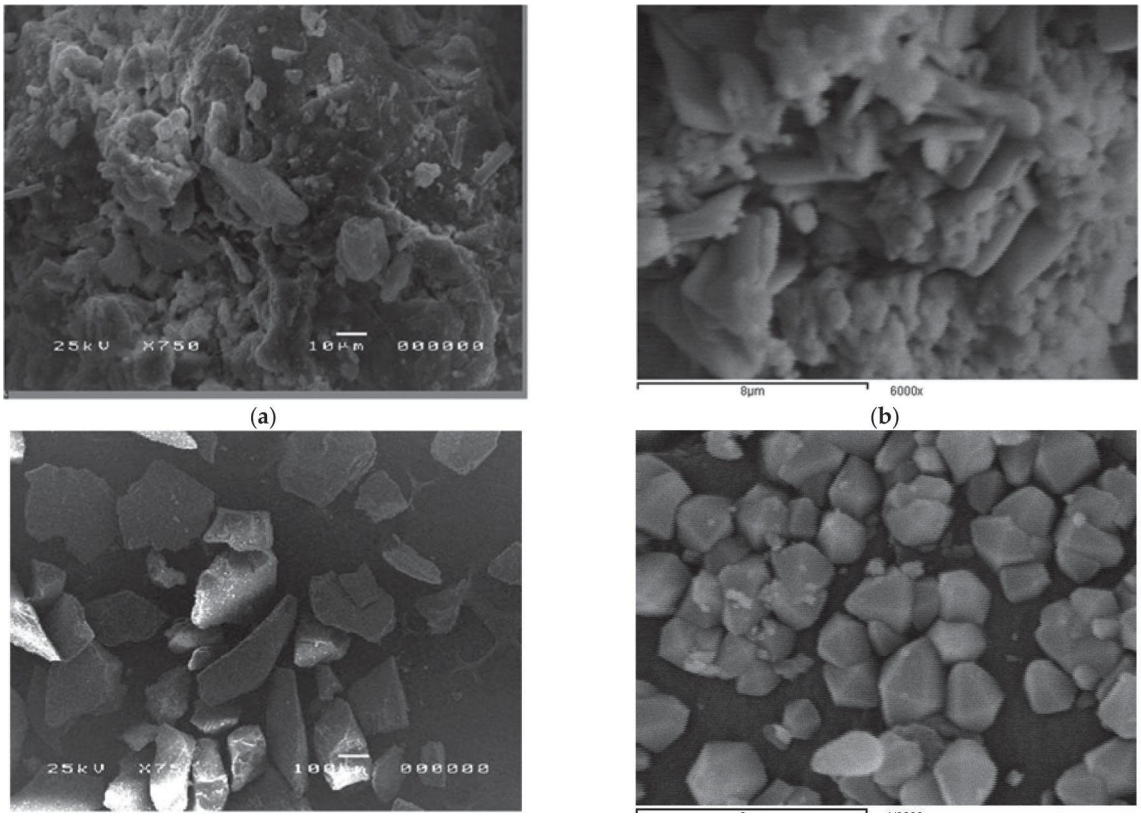

(**a**) (**b**)

Fig. 1. Scanning electron microscope (SEM) images of natural, synthetic, and nanocomposite silica (**a**): natural silica; (b): natural Fe_2O_3/ SiO_2 nanocomposite; (**c**): synthetic TEOS (**d**): synthetic Fe_2O_3/ TEOS nanocomposite.

porosity by nitrogen adsorption/desorption isotherm using the BJH. We found that the surface area of natural silica nanocomposite was (43.12 m^2/ g) smaller than the synthetic one (320 m^2/ g). So we can expect a decrease in the interaction between natural silica nanocomposite and heavy metals.

The EDX elemental composition of the drinking water and the adsorption efficiency (AE) and the adsorption capacity (AQ), of the natural, synthetic, and nanocomposite silica for heavy metals

Table 2 displays the EDX elemental composition (mg/l) in the prepared drinking water before and after cleaning with 0.5, 1% natural, synthetic, and nanocomposite silica. The general trend of the EDX elemental composition (mg/l) is as shown contaminated water > natural Fe_2O_3/ SiO_2 nanocomposite (0.5%) > synthetic silica TEOS (0.5%) > natural Fe_2O_3/ SiO_2 nanocomposite (1%) > synthetic Fe_2O_3/ TEOS nanocomposite (0.5%) > synthetic Fe_2O_3/ TEOS nanocomposite (1%) > synthetic silica TEOS (1%) > natural silica SiO_2 (0.5%) > natural silica SiO_2 (1%) > purified water. It can be inferred that the lowest $P \leq 0.05$ composition of Mn^{2+}, Fe^{2+}, Ni^{2+}, Hg^{2+}, and Pb^{2+} were found in contaminated water treated with natural silica SiO_2 (1%, 0.5%), however the highest $P \leq 0.05$ elemental composition were found to be in the Fe_2O_3/ SiO_2 nanocomposite (0.5, 1%), followed by synthetic TEOS (0.5%). These results could be explained more clearly within the amounts of heavy metal ions removed, after water cleaning, per unit mass of natural, synthetic, and nanocomposite silica (Figure 2 and 3). Adsorbent concentration is an important parameter in the adsorption of heavy metal ions from contaminated water owing to its effects on the amounts of heavy metal ions removed per unit mass of adsorbent (Kukwa *et al.*, 2020). In the present work, the percentages of heavy metals removed were increased with the increasing mass of the natural, synthetic, and nanocomposite silica from 5 to 10 g (Fig. 2). The natural silica SiO_2 at 0.5 and 1% exhibited efficient removal up to 97.05%, and complete removal of 100% for Zn^{2+}, Fe^{2+}, and Ni^{2+}, respectively, as it affected by its superior microstructure (Fig. 1 a) with high concentrations of Si—OH groups coupled with ordered cristobalite amorphous structures, and the non-uniform pore sizes, make natural silica efficient sorbent for complete removal of Zn^{2+}, Fe^{2+}, and Ni^{2+} (Basri *et al.*, 2020). Also, synthetic Fe_2O_3/ TEOS nanocomposite

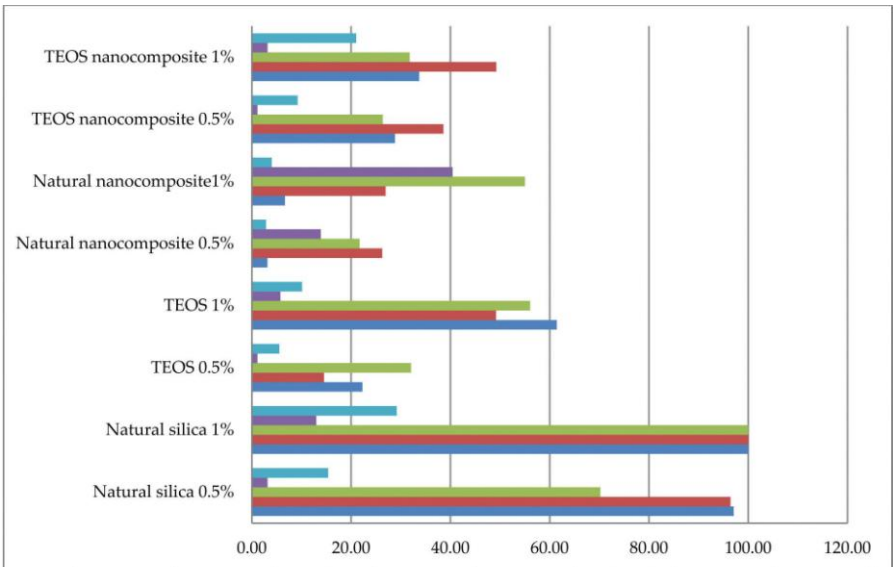

	Natural silica 0.5%	Natural silica 1%	TEOS 0.5%	TEOS 1%	Natural nanocompo site 0.5%	Natural nanocompo site1%	TEOS nanocompo site 0.5%	TEOS nanocompo site 1%
Pb	15.36	29.19	5.55	10.11	2.84	4.01	9.23	21.01
Hg	3.16	12.99	1.12	5.75	13.89	40.42	1.12	3.16
Ni	70.21	100.00	32.04	56.04	21.70	55.02	26.38	31.79
Fe	96.40	100.00	14.53	49.19	26.25	26.94	38.59	49.24
Mn	97.05	100.00	22.27	61.44	3.14	6.68	28.84	33.70

Fig. 2. Adsorption efficiency (AE, %) for heavy metals of the natural, synthetic, and nanocomposite silica

Table 2. EDX elemental composition (mg/ L) in the prepared drinking water before and after cleaning with natural, synthetic, and nanocomposite silica

Heavy metals	Purified water	Contaminated water	Natural silica SiO_2		Synthetic silica TEOS		Natural Fe_2O_3/ SiO_2 nanocomposite		Synthetic Fe_2O_3/ TEOS nanocomposite	
			0.5%	1%	0.5%	1%	0.5%	1%	0.5	1%
Mn	ND	151.73±0.3^{a}	4.47±0.95^{e}	ND	117.94±1.1^{b}	58.5±2.1^{d}	146.97±0.64^{a}	141.6±0.51^{ab}	107.97±2.0^{c}	100.6±1.25^{c}
Fe	ND	280.20±5.2^{a}	10.08±0.23^{e}	ND	239.48±1.6^{ab}	142.36±1.8^{d}	206.64±1.8^{b}	204.72±5.3^{b}	172.08±1.4^{cb}	142.24±0.15^{d}
Ni	ND	2.35±1.4^{a}	0.7±0.6^{d}	ND	1.59±0.49^{ab}	1.03±0.63^{c}	1.84±0.18^{ab}	1.06±0.84^{c}	1.73±0.69^{ab}	1.60±0.6^{ab}
Hg	ND	0.48±0.64^{a}	0.46±1.5^{a}	0.41±0.52^{a}	0.46±1.6^{a}	0.45±0.13^{a}	0.41±0.44^{a}	0.28±0.16^{b}	0.47±0.88^{a}	0.46±0.53^{a}
Pb	ND	10.22±3.0^{a}	8.65±1.1^{b}	7.24±1.37^{d}	9.65±0.94^{ab}	9.19±0.94^{b}	9.93±1.1^{ab}	9.81±0.99^{ab}	9.28±2.3^{b}	8.07±0.8^{c}

ND: not detected.

Data are presented as means ± SDM (n=3) & Means within a column with different letters are significantly different at $P \leq 0.05$.

Table 3. Serum biomarkers of rat kidney treated with the prepared drinking water.

Serum biomarkers	Purified water	Contaminated water	Natural silica SiO_2		Synthetic silica TEOS		Natural Fe_2O_3/ SiO_2 nanocomposite		Synthetic Fe_2O_3/ TEOS nanocomposite	
			0.5%	1%	0.5%	1%	0.5%	1%	0.5	1%
Urea	39.3±1.52^{f}	87.0±2.0^{a}	39.3±0.57^{f}	39.0±1.0^{f}	45.3±1.15^{e}	41.6±1.15^{ef}	67.3±2.08^{b}	55.6±1.15^{c}	51.6±1.15^{d}	49.3±1.15^{d}
Creatinine	0.76±0.1^{f}	2.2±0.2^{a}	0.76±0.1^{f}	0.73±0.1^{f}	1.23±0.1^{cd}	1.06±0.1^{e}	1.86±0.1^{b}	1.76±0.1^{b}	1.51±0.1^{c}	1.36±0.1^{c}
Uric acid	3.56±0.1^{e}	8.3±0.2^{a}	3.76±0.2^{e}	3.66±0.2^{e}	6.1±0.12^{c}	5.23±0.2^{d}	7.1±0.2^{b}	6.8±0.1^{b}	6.2±0.3^{c}	5.73±0.2^{c}

Data are presented as means ± SDM (n=5) & Means within a column with different letters are significantly different at $P \leq 0.05$.

at 0.5 and 1% was more efficient than natural Fe_2O_3/ SiO_2 nanocomposite in removing Mn^{2+}, Fe^{2+}, Ni^{2+}, and Pb^{2+} . The maximum percentages were 33.70, 49.24, 31.79, and 21.01%, respectively. These results owing to that the surface area of Fe_2O_3/ SiO_2 nanocomposite (Fig.1b) was decreased as affected by the aggregation of Fe_2O_3 and the Van der Waals forces (Ramutshatsha-Makhwedzha *et al.*, 2019). In our early study (Reda *et al.*, 2018), we found that the surface area of natural silica nanocomposite was (43.12 m^2/ g) smaller than the synthetic one (320 m^2/ g). But what is worth that the natural Si_2O_3 nanocomposite 1% has specific priority and selectivity to bind certain types of metal depending upon above- mentioned aggregations and Van der Waals forces (Aliyah, 2012), where it showed the highest efficiency for removing Hg^{2+} with a maximum percentage of 40.42%.

The results in Figure 3 exhibited a reverse relationship—the adsorption capacity (AQ, mg/ g) was decreased when the silica mass increased from 5 to 10 g. For example; 0.5% natural silica adsorbed more Mn^{2+} (29.45 mg/ g), and Fe^{2+} (54.02 mg/ g) than Mn^{2+} (15.17 mg/ g), and Fe^{2+} (28.02 mg/ g) for 1% natural silica. This result was due to the saturation of accessible active sites on sorbent materials above a certain concentration of heavy metals (Gorzin *et al.*, 2018; Abdel Halim *et al.*, 2019). It can be inferred that the higher composition of coexisting heavy metals in the contaminated water resulted in the stronger competition among heavy metals, where the elemental composition of Fe^{2+} (280.20±5.2 mg/L) was higher than Ni^{2+} (2.35±1.4), and Hg^{2+} (0.48±0.64) (Table 2), so Fe^{2+} could compete with Ni^{2+} and Hg^{2+} to be adsorbed more on the surface of the natural silica. Another reason may be related to the ionic radius of heavy metals, where the atomic radius of Fe (0.126 nm) < Hg (0.3150 nm) < Ni (0.3163 nm), the lower atomic radius, lower hydration energy of the heavy metals was easier for the adsorption (Ouyang *et al.*, 2019).

Serum biomarkers for rat kidney function

Table 3 represents the serum biomarkers of

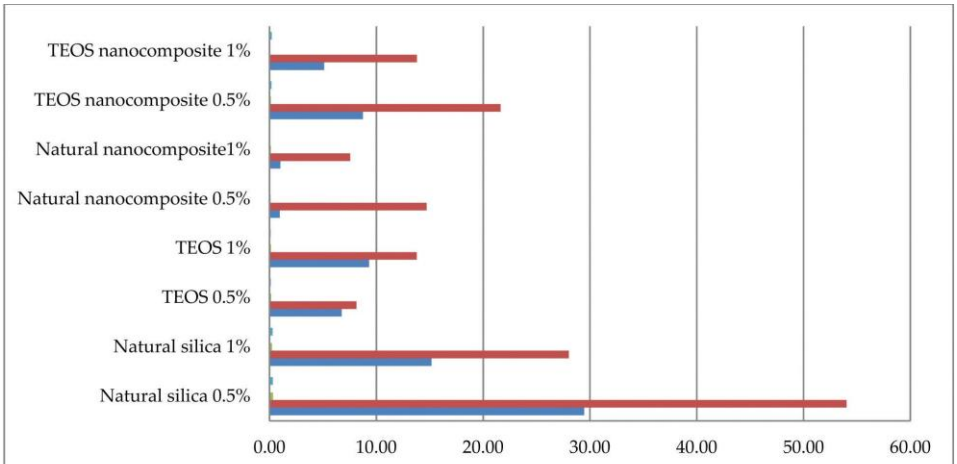

	Natural silica 0.5%	Natural silica 1%	TEOS 0.5%	TEOS 1%	Natural nanocompo site 0.5%	Natural nanocompo site1%	TEOS nanocompo site 0.5%	TEOS nanocompo site 1%
Pb	0.31	0.30	0.11	0.10	0.06	0.04	0.19	0.21
Hg	0.00	0.01	0.00	0.00	0.01	0.02	0.00	0.00
Ni	0.33	0.24	0.15	0.13	0.10	0.13	0.12	0.07
Fe	54.02	28.02	8.14	13.78	14.71	7.55	21.62	13.80
Mn	29.45	15.17	6.76	9.32	0.95	1.01	8.75	5.11

Fig. 3. Adsorption capacity (AQ, mg/ g) for heavy metals of the natural, synthetic, and nanocomposite silica

rat kidneys fed the prepared drinking water. There were significant ($p \leq 0.05$) alterations in the levels of serum urea, creatinine, and uric acid in rats exposed to drinking water contaminated with heavy metals, compared to the rats exposed to purified water. On the other hand, both natural silica SiO_2 (0.5, 1%) and synthetic TEOS (1%) exhibited close results to the normal values observed in rats exposed to purified water. In comparison, synthetic Fe_2O_3/ TEOS nanocomposite at concentrations 0.5 and 1% showed better results than Fe_2O_3/ SiO_2 nanocomposites at the same concentrations. These results are coherent with the results in Table 2 and Fig. (1b & d), where synthetic Fe_2O_3/ TEOS nanocomposite had a larger surface area (Fig. 1d) and higher efficiency in the adsorption of heavy metals than natural Fe_2O_3/ SiO_2 nanocomposite (Fig. 2), as well as natural silica SiO_2 had higher efficiency in the adsorption of heavy metals than Synthetic silica TEOS (Fig. 2).

There are controversial results regarding serum biomarkers in the experimental trials. A group of researchers (Oyagbemi *et al.*, 2015) found that oral administration of Pb $(CH_3COO)_2$ in rats caused $p <$ 0.01 increase in the blood urea and serum creatinine, most likely happened in acute and chronic intrinsic renal disease, and also when there was a decrease in the effective circulating blood volume with a decrease in renal perfusion (Basile *et al.*, 2012). While another group (Waghmare *et al.*, 2015) found that serum urea was reduced in all rat groups treated with Ni^{+2}, Fe^{+2}, and Mn^{+2}. Also, Andjelkovic et al. (2019) found that acute exposure to Cd^{+2} and Pb^{+2} administered alone or in a mixture form resulted in ($p < 0.01$) decreased urea concentrations, while there was a slight ($p < 0.01$) increase in creatinine levels compared to the control group. On the other hand, Wang *et al*. (2020) found no significant changes in the biochemical parameters included urea, creatinine, and uric acid in experimental animals fed a multi-heavy metal mixture with 500 mg/ kg body weight for six months, compared to untreated animals. The authors stated that the kidney might still be in a compensatory stage, while the heavy metals were accumulated in different degrees in the kidney.

Histology of rat kidney

Figure 4 (a-j) displays the histopathological sections of kidneys for male rats of various studied groups. The kidney section of the rats exposed to purified water (Fig. 4a) showed the normal structure of renal parenchyma, normal podocytes, normal glomerular capillaries with thin and delicate loops, normal number of the endothelial cells, and normal

surrounding tubules. However, the kidney section of the rats exposed to contaminated water with heavy metals (Fig. 4 b) showed sever histopathological changes, including necrosis and degeneration of the renal tubules, interstitial fibrosis, hypertrophy, and hemorrhage (Albu *et al.*, 2021). Hypertrophy is characterized by an increase in the Bowman's Space, expansion of the connective tissues, and shrank of the glomerulus. The hemorrhage is accompanied by vacuolization of the epithelial cells, a deposit of the RBCs and clogged blood vessels in the capillaries, and decreased hematopoietic tissue (Riaz *et al.*, 2020). These histological changes could be explained as; heavy metals-induced nephrotoxicity is mediated by rapid selective accumulation of heavy metals and metalloid complexes which are filtrated by kidney glomerulus, taken up by the cytosolic fraction of proximal tubular epithelium and leads to gradual loss of the kidney function and tissue damage (Abd El-Rahman *et al.*, 2016; Seif *et al.*, 2019).

The kidney section of the rats exposed to contaminated water treated with 0.5, 1% natural silica (Fig.4 c & d), and 1% synthetic TEOS (Fig. 4 f) do not exhibit any sign of nephrotoxicity either hemorrhage or tissue damage; they were most likely similar to that section for the rats exposed to purified water. Meanwhile, the kidney section of the rats exposed to contaminated water treated with 0.5% synthetic TEOS (Fig. 4 e) exhibited renal tissue completely normal, except for mild degeneration in the dilated capillaries and the lining epithelium of the proximal and distal tubules (Seif *et al.*, 2019).

The kidney section of the rats exposed to contaminated water treated with 0.5% Fe_2O_3/ SiO_2 nanocomposite showed cystic dilatation of renal

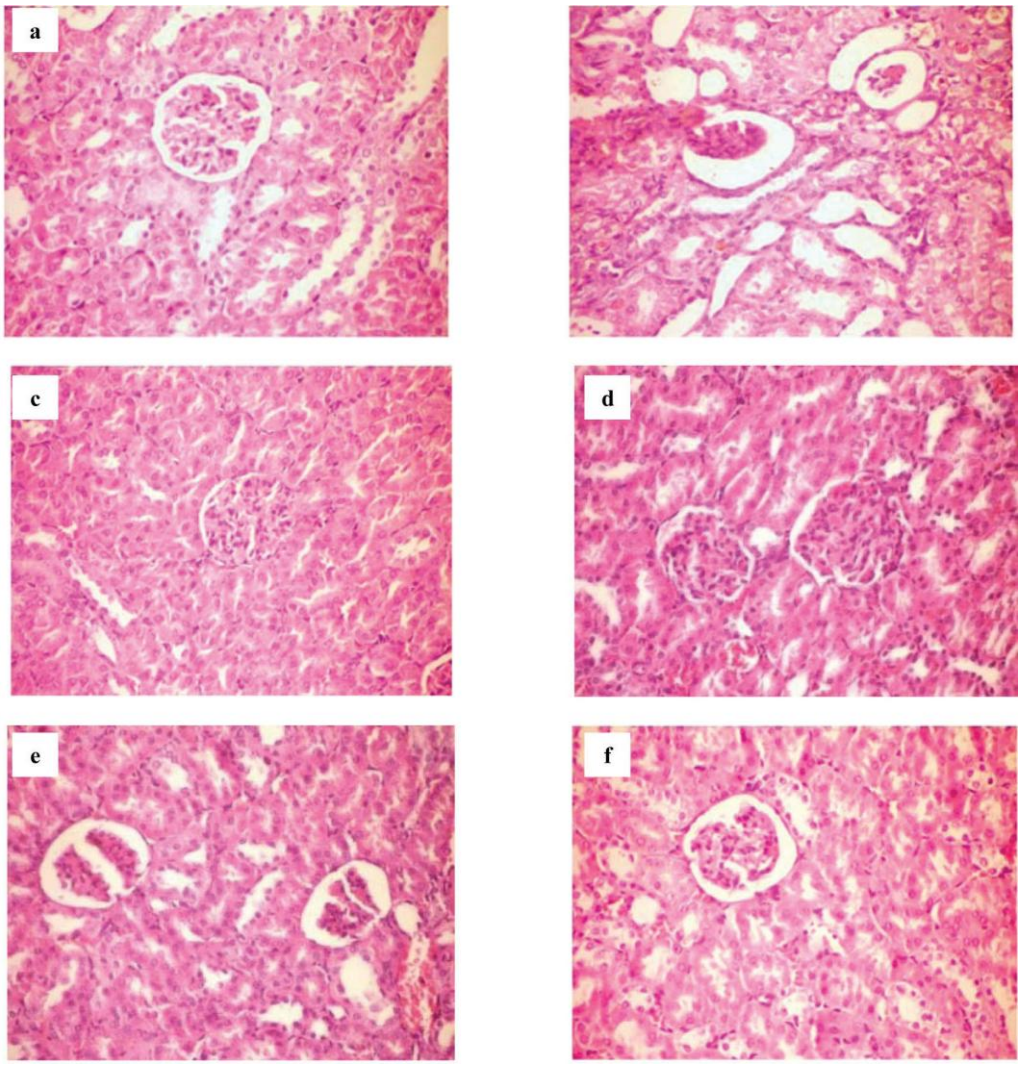

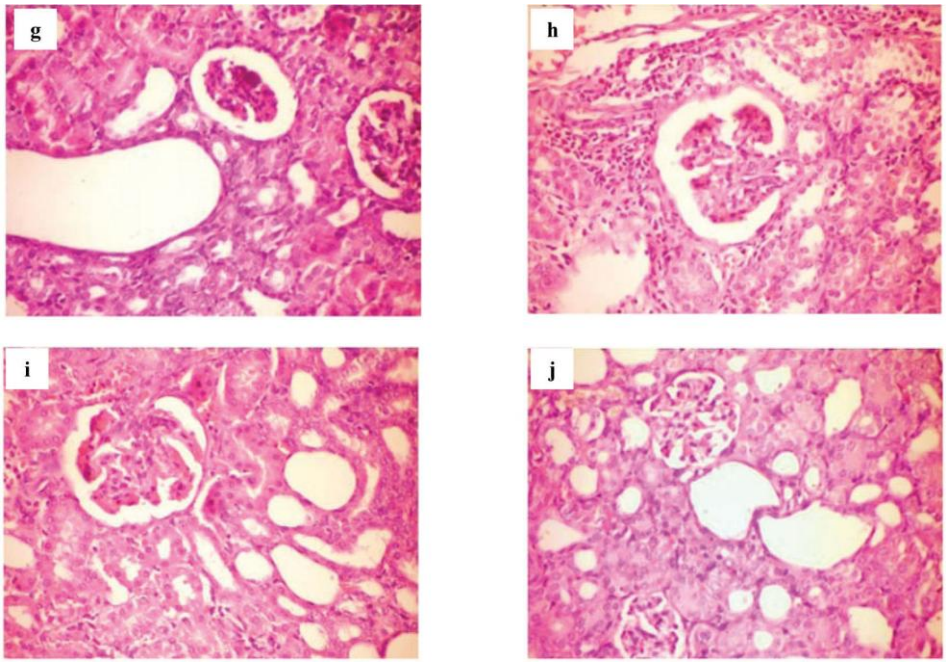

Fig. 4. Histological sections of renal rat exposed to different drinking water (Stained with H&E, 200×). (**a**) Purified water. (**b**) Contaminated water with heavy metals. (**c**) Contaminated water treated with 0.5% natural silica. (**d**) Contaminated water treated with 1% natural silica. (**e**) Contaminated water treated with o.5% synthetic TEOS. (**f**) Contaminated water treated with 1% synthetic TEOS. (**g**) Contaminated water treated with 0.5% Fe_2O_3/ SiO_2 nanocomposite. (**h**) Contaminated water treated with 1% Fe_2O_3/ SiO_2 nanocomposite. (**i**) Contaminated water treated with 0.5% synthetic Fe_2O_3/ TEOS nanocomposite. (j) Contaminated water treated with 1% synthetic Fe_2O_3/ TEOS nanocomposite.

tubules and atrophy of some glomerulus (Fig. 4 g). In addition to these histological changes, the kidney section of the rats exposed to contaminated water treated with 1% Fe_2O_3/ SiO_2 nanocomposite (Fig. 4 h) showed thickening of the parietal layer of Bowman's capsule and local interstitial nephritis. In a study done by Mehdi *et al.* (2021), rats exposed to 100 & 150 mg/kg silica nanoparticles showed necrosis, infiltration, dilation, and vacuolation in renal tissues and tubules with significant degrees of alterations.

The kidney section of the rats exposed to contaminated water treated with 0.5% synthetic Fe_2O_3/ TEOS nanocomposite (Fig. 4 i) showed congestion of glomerular tuft and cystic dilatation of renal tubules. However, 1% synthetic Fe_2O_3/ TEOS nanocomposite (Fig. 4 j) showed cystic dilatation and vacuoles within tubules, without atrophy or necrosis (Boudard *et al.*, 2019).

CONCLUSION

Water contamination with co-existing heavy metals could be partially controlled via converting rice husk as underutilized horticultural biomass, into silica and Fe_2O_3 silica nanocomposite using the sol-gel method. Silica, with its inspiring morphology and mass of 5 g, completely removed 151.73 mg Zn^{2+}, 280.20 mg Fe^{2+}, and 2.35 mg Ni^{2+}/ L of contaminated water, as confirmed by the SEM and EDX tools. The more achievable results in this study that each 10 g mass of Fe_2O_3 silica nanocomposite with its aggregations and Van der Waals forces showed strong affinity and selectivity to bind 40.42% of Hg^{2+}/ L of contaminated water with co-existing heavy metals. The described solution can be more economical and environmentally alternative than synthesized TEOS or Fe_2O_3/ TEOS nanoparticle, which may not be sustainable and not match the health and the cost requirements. Based on a combination of serum biomarkers and histological examination for serum and renal tissues, there were no significant alterations or any indications of nephrotoxicity in rats exposed to contaminated water treated with 0.5, 1% natural silica.

Funding

"This research received no external funding."

ACKNOWLEDGMENT

The authors acknowledged the Pathology Department, Faculty of Veterinary Medicine, Cairo University, Al Giza, Egypt for the technical support and the materials used in the histopathological examination of kidney.

Conflicts of Interest

"The authors declare no conflict of interest."

REFERENCES

Abd El-Rahman, N.A., Saad, A.M., Walid, M.S. and Afaf, A.A.S. 2016. Preventive effect of black rice ethanolic extract as natural antioxidants on some heavy metals induced disorders in experimental animal. Int. J. Food, Nutrition and Public Health. 8 (1) : 20-34.

Abdel Halim, A., El-Ezaby, K. and El-Gammal, M. 2019. Removal of Fe^{2+} and Pb^{2+} ions from wastewater using rice husks-based adsorbents. Journal of Egyptian Academic Society for Environmental Development. D, Environmental Studies. 20(1) : 47-60.

Agi, A., Junin, R., Jaafar, M. Z., Mohsin, R., Arsad, A., Gbadamosi, A. and Gbonhinbor, J. 2020. Synthesis and application of rice husk silica nanoparticles for chemical enhanced oil recovery. Journal of Materials Research and Technology. 9(6) : 13054-13066.

Albu, P., Herman, H., Balta, C., Lazar, V., Fulop, A., Baranyai, E. and Dinischiotu, A. 2021. Correlation between Heavy Metal-Induced Histopathological Changes and Trophic Interactions between Different Fish Species. Applied Sciences. 11(9) : 3760.

Aliyah Nurul Akma. Adsorption of lead using rice husk. 2012. PhD Thesis. UMP.

Andjelkovic, M., Buha Djordjevic, A., Antonijevic, E., Antonijevic, B., Stanic, M., Kotur-Stevuljevic, J. and Bulat, Z. 2019. Toxic effect of acute cadmium and lead exposure in rat blood, liver, and kidney. International Journal of Environmental Research and Public Health. 16(2) : 274.

Basile, D. P., Anderson, M. D. and Sutton, T. A. 2012. Pathophysiology of acute kidney injury Comprehensive Physiology. 2(2) : 1303.

Basri, M. S. M., Mustapha, F., Mazlan, N. and Ishak, M. R. 2020. Optimization of rice husk ash-based geopolymers coating composite for enhancement in flexural properties and microstructure using response surface methodology. Coatings. 10(2) : 165.

Boudard, D., Aureli, F., Laurent, B., Sturm, N., Raggi, A., Antier, E. and Bencsik, A. 2019. Chronic oral exposure to synthetic amorphous silica (NM-200) results in renal and liver lesions in mice. Kidney International Reports. 4(10) : 1463-1471.

Candido, I. C. M., Pires, I. C. B. and de Oliveira, H. P. 2021. Natural and Synthetic Fiber-Based Adsorbents for Water Remediation. CLEAN-Soil, Air, Water. 49 : 2000189.

Dang, N. T. T., Nguyen, T. T. A., Phan, T. D., Tran, H., Van Dang, P. and Nguyen, H. Q. 2017. Synthesis of silica nanoparticles from rice husk ash. Science and Technology Development Journal. 20(K7) : 50-54.

FAOSTAT 2019. Food and Agriculture Organization of the United Nations: Crops and livestock products. Available online: https://www.fao.org/faostat/en/#data/QCL

Gorzin, F. and Bahri Rasht Abadi, M. M. 2018. Adsorption of Cr (VI) from aqueous solution by adsorbent prepared from paper mill sludge: Kinetics and thermodynamics studies. Adsorption Science & Technology. 36(1-2) : 149-169.

Hrianca, I., Caizer, C., Savii, C. and Popovici, M. 2000. Magnetic and Structural Properties of ã-Fe_2O_3 nanoparticles dispersed in silica matrix. Journal of Optoelectronics and Advanced Materials. 2(5) : 634-638.

Hu, X. E., Luo, X., Xiao, G., Yu, Q., Cui, Y., Zhang, G. and and Zeng, Z. 2020. Low-cost novel silica@ polyacrylamide composites: fabrication, characterization, and adsorption behavior for cadmium ion in aqueous solution. Adsorption. 26(7): 1051-1062.

Jaishankar, M., Tseten, T., Anbalagan, N., Mathew, B. B., and Beeregowda, K. N. 2014. Toxicity, mechanism and health effects of some heavy metals. Interdisciplinary Toxicology. 7(2) : 60-72.

Kamath, S. R. and Proctor, A. 1998. Silica gel from rice hull ash: preparation and characterization. Cereal Chemistry. 75(4) : 484-487.

Khan, M. S., Javed, M., Rehman, M. T., Urooj, M. and Ahmad, M. I. 2020. Heavy metal pollution and risk assessment by the battery of toxicity tests. Scientific Reports. 10(1) : 1-10.

Kukwa, R. E., Kukwa, D. T., Oklo, A. D., Ligom, T. T., Ishwah, B. and Omenka, J. A. 2020. Adsorption Studies of Silica Adsorbent Using Rice Husk as a Base Material for Metal Ions Removal from Aqueous Solution. American Journal of Chemical Engineering, 8(2) : 48-53.

Ligate, F. J. and Mdoe, J. E. 2015. Removal of heavy metal ions from aqueous solution using rice husks-based adsorbents. Tanzania Journal of Science. 41(1) : 90-102.

Masoud, M. S., El-Saraf, W. M., Abdel-Halim, A. M., Ali, A. E., Mohamed, E. A. and Hasan, H. M. 2016. Rice husk and activated carbon for waste water treatment of El-Mex Bay, Alexandria Coast, Egypt. Arabian Journal of Chemistry. 9 : S1590-S1596.

Mehdi, L. A. and Al-Husseini, A. M. H. 2021. Estimate Toxic Effect of Silica Nanoparticles on Kidney, Liver and Lung Function of Male Albino Rats. Systematic Reviews in Pharmacy. 12(3) : 136-141.

National Research Council. 1995. Nutrient requirements of laboratory animals: 1995.

Nguyen, T. T., Ma, H. T., Avti, P., Bashir, M. J., Ng, C. A., Wong, L. Y. and Tran, N. Q. 2019. Adsorptive removal of Iron using SiO_2 nanoparticles extracted from rice husk ash. Journal of Analytical Methods in Chemistry, 2019: 1-9.

Nwokocha, C., Ejebe, D., Nwangwa, E., Ekene, N., Akonoghrere, R. and Ukwu, J. 2010. The effects of bitter kola supplemented diet on hepatotoxicity of mercury in Wistar rats. Journal of Applied Sciences and Environmental Management. 14(1).

Ong, H. R., Iskandar, W. M. E. and Khan, M. M. R. 2019. Rice Husk Nanosilica Preparation and Its Potential Application as Nanofluids. In Engineered Nanomaterials-Health and Safety. IntechOpen. https://doi.org/10.5772/intechopen.89904.

Ouyang, D., Zhuo, Y., Hu, L., Zeng, Q., Hu, Y. and He, Z. 2019. Research on the adsorption behavior of heavy metal ions by porous material prepared with silicate tailings. Minerals. 9(5) : 291.

Oyagbemi, A. A., Omobowale, T. O., Akinrinde, A. S., Saba, A. B., Ogunpolu, B. S. and Daramola, O. 2015. Lack of reversal of oxidative damage in renal tissues of lead acetate-treated rats. Environmental Toxicology. 30(11) : 1235-1243.

Palanivelu, R., Manivasakan, P., Dhineshbabu, N. R. and Rajendran, V. 2016. Comparative study on isolation and characterization of amorphous silica nanoparticles from different grades of rice hulls. Synthesis and Reactivity in Inorganic, Metal-Organic, and Nano-Metal Chemistry. 46(3) : 445-452.

Ramutshatsha-Makhwedzha, D., Ngila, J. C., Ndungu, P. G. and Nomngongo, P. N. 2019. Ultrasound Assisted Adsorptive Removal of Cr, Cu, Al, Ba, Zn, Ni, Mn, Co and Ti from Seawater Using Fe_2O_3-SiO_2-PAN Nanocomposite: Equilibrium Kinetics. Journal of Marine Science and Engineering. 7(5) : 133.

Reda, S., AL-Ghannam, S. M. and Abd El-Rahman, S. N. 2018. Effect of Source of Silica on Properties of Fe_2O_3/SiO_2 Nanocompsites and Their Application on Hepatic Injury in Rats as Adsorbents for Removal of Heavy Metal from Drinking Water. Asian Journal of Chemistry. 30(3) : 625-632.

Rehman, K., Fatima, F., Waheed, I. and Akash, M. S. H. 2018. Prevalence of exposure of heavy metals and their impact on health consequences. Journal of Cellular Biochemistry. 119(1) : 157-184.

Riaz, M. A., Nisa, Z. U., Anjum, M. S., Butt, H., Mehmood, A., Riaz, A. and Akhtar, A. B. T. 2020. Assessment of metals induced histopathological and gene expression changes in different organs of non-diabetic and diabetic rats. Scientific Reports. 10(1): 1-11.

Seif, M. M., Madboli, A. N., Marrez, D. A. and Aboulthana, W. M. 2019. Hepato-renal protective effects of Egyptian purslane extract against experimental cadmium toxicity in rats with special emphasis on the functional and histopathological changes. Toxicology Reports. 6 : 625-631.

Siddique, R. and Cachim, P. 2018. Waste and Supplementary Cementitious Materials in Concrete: Characterisation, Properties and Applications. Woodhead Publishing.

Suvarna, K. S., Layton, C. and Bancroft, J. D. (Eds.). 2018. Bancroft's theory and practice of histological techniques E-Book. Elsevier Health Sciences.þ

Thiedeitz, M., Schmidt, W., Härder, M. and Kränkel, T. 2020. Performance of rice husk ash as supplementary cementitious material after production in the field and in the lab. Materials. 13(19) : 4319.

Vieira, M. G. A., de Almeida Neto, A. F., Da Silva, M. G. C., Carneiro, C. N. and Melo Filho, A. A. 2014. Adsorption of lead and copper ions from aqueous effluents on rice husk ash in a dynamic system. Brazilian Journal of Chemical Engineering. 31 : 519-529.

Waghmare, T. E., Nayaka, H. B., Banklgi, S. K. C. and Tukappa, A. 2015. Quantitative estimation of heavy metals in river water and their toxicity, hematology, gravimetric, serum and tissue biochemistry effects in albino rats. World Journal of Pharmaceutical Research. 4(2) : 1415-1425.

Wang, W., Martin, J. C., Fan, X., Han, A., Luo, Z. and Sun, L. 2012. Silica nanoparticles and frameworks from rice husk biomass. ACS Applied Materials and Interfaces. 4(2) : 977-981.

Wang, Y., Tang, Y., Li, Z., Hua, Q., Wang, L., Song, X. and Tang, C. 2020. Joint toxicity of a multi-heavy metal mixture and chemoprevention in Sprague Dawley rats. International Journal of Environmental Research and Public Health. 17(4) : 1451.

Wasana, H. M., Perera, G. D., Gunawardena, P. D. S., Fernando, P. S. and Bandara, J. 2017. WHO water quality standards Vs Synergic effect (s) of fluoride, heavy metals and hardness in drinking water on kidney tissues. Scientific Reports. 7(1) : 1-6.

Water, (U. N. 2018). 2018 UN World Water Development Report, Nature-based Solutions for Water.

World Health Organization. 2006. A compendium of drinking water quality standards in the Eastern Mediterranean Region (No. WHO-EM/CEH/143/E). 1-18.